Experimental report

12/02/2018

Proposal: **4-01-1472** **Council:** 4/2015

Title: Magnetic excitation spectrum of the Helimagnetic Spinel compound ZnCr2Se4

Research area: Physics

This proposal is a new proposal

Main proposer: **Alistair CAMERON**

Experimental team:
Alexander SUKHANOV
Yevhen ONYKIIENKO
Yuliia TYMOSHENKO
Dmytro INOSOV
Alistair CAMERON

Local contacts:
Alexandre IVANOV
Andrea PIOVANO

Samples: ZnCr2Se4

Instrument	Requested days	Allocated days	From	To
IN8	8	4	27/02/2017	03/03/2017

Abstract:

ZnCr2Se4 is a magnetically frustrated spinel compound with an incommensurate ground state. At low temperatures it displays a spin spiral structure propagating along the (100) crystal directions, and the formation of this state is accompanied by a structural transition, indicating a spin-lattice coupling. With our sample of co-alligned single crystals, we propose to map out the magnetic excitation spectrum of this compound and by doing so quantitatively determine the strength of the magnetic interactions, with the aim of developing a realistic magnetic Hamiltonian for this material. To do this we request 8 days of beamtime on the IN8 spectrometer.

PHYSICAL REVIEW X **7,** 041049 (2017)

Pseudo-Goldstone Magnons in the Frustrated $S = 3/2$ Heisenberg Helimagnet $ZnCr_2Se_4$ with a Pyrochlore Magnetic Sublattice

Y. V. Tymoshenko,[1] Y. A. Onykiienko,[1] T. Müller,[2] R. Thomale,[2] S. Rachel,[3] A. S. Cameron,[1]
P. Y. Portnichenko,[1] D. V. Efremov,[4] V. Tsurkan,[5,6] D. L. Abernathy,[7] J. Ollivier,[8]
A. Schneidewind,[9] A. Piovano,[8] V. Felea,[6] A. Loidl,[5] and D. S. Inosov[1,*]

[1]*Institut für Festkörper- und Materialphysik, Technische Universität Dresden,*
D-01069 Dresden, Germany
[2]*Institut für Theoretische Physik, Universität Würzburg, 97074 Würzburg, Germany*
[3]*Institut für Theoretische Physik, Technische Universität Dresden, D-01062 Dresden, Germany;*
Department of Physics, Princeton University, Princeton, New Jersey 08544, USA;
School of Physics, University of Melbourne, Parkville, Victoria 3010, Australia
[4]*Institute for Theoretical Solid State Physics, IFW Dresden,*
Helmholtzstraße 20, D-01069 Dresden, Germany
[5]*Experimental Physics V, Center for Electronic Correlations and Magnetism,*
Institute of Physics, University of Augsburg, D-86135 Augsburg, Germany
[6]*Institute of Applied Physics, Academy of Sciences of Moldova, Chisinau MD-2028, Republic of Moldova*
[7]*Quantum Condensed Matter Division, Oak Ridge National Laboratory,*
Oak Ridge, Tennessee 37831, USA
[8]*Institut Laue-Langevin, 71 avenue des Martyrs, CS 20156, F-38042 Grenoble cedex 9, France*
[9]*Jülich Center for Neutron Science (JCNS), Forschungszentrum Jülich GmbH,*
Outstation at Heinz Maier–Leibnitz Zentrum (MLZ), Lichtenbergstraße 1,
D-85747 Garching, Germany

(Received 12 May 2017; published 29 November 2017)

Low-energy spin excitations in any long-range ordered magnetic system in the absence of magnetocrystalline anisotropy are gapless Goldstone modes emanating from the ordering wave vectors. In helimagnets, these modes hybridize into the so-called helimagnon excitations. Here we employ neutron spectroscopy supported by theoretical calculations to investigate the magnetic excitation spectrum of the isotropic Heisenberg helimagnet $ZnCr_2Se_4$ with a cubic spinel structure, in which spin-3/2 magnetic Cr^{3+} ions are arranged in a geometrically frustrated pyrochlore sublattice. Apart from the conventional Goldstone mode emanating from the $(0\,0\,q_h)$ ordering vector, low-energy magnetic excitations in the single-domain proper-screw spiral phase show soft helimagnon modes with a small energy gap of ~0.17 meV, emerging from two orthogonal wave vectors $(q_h\,0\,0)$ and $(0\,q_h\,0)$ where no magnetic Bragg peaks are present. We term them pseudo-Goldstone magnons, as they appear gapless within linear spin-wave theory and only acquire a finite gap due to higher-order quantum-fluctuation corrections. Our results are likely universal for a broad class of symmetric helimagnets, opening up a new way of studying weak magnon-magnon interactions with accessible spectroscopic methods.

DOI: 10.1103/PhysRevX.7.041049

Subject Areas: Condensed Matter Physics, Magnetism,
Strongly Correlated Materials

I. INTRODUCTION

A. Classical Heisenberg model on the pyrochlore lattice

The Heisenberg model on the pyrochlore lattice attracts a lot of interest as various spin models on this lattice give rise to the simplest three-dimensional frustrated spin systems. Even for classical spins, this model hosts a wide range of different ground states. Considering only the antiferromagnetic nearest-neighbor (NN) interactions results in a classical spin liquid [1], exhibiting no long-range magnetic order down to zero temperature. This is explained by strong geometric frustration that leads to a highly degenerate classical ground state. However, inclusion of further-neighbor interactions relieves this frustration and stabilizes various ordered ground states, among them ferromagnetism, single- or multi-**q** spin spirals, nematic order, and other exotic phases [2–6].

Chromium spinels provide great opportunities to investigate magnetic interactions between classical spins on the

---

[*] Corresponding author.
dmytro.inosov@tu-dresden.de

structurally ideal pyrochlore lattice. These compounds have the general formula ACr_2X_4, where A and X are nonmagnetic ions and Cr^{3+} is the magnetic cation in the $3d^3$ configuration [7]. Its magnetic sublattice has the pyrochlore structure with spins $S = 3/2$ at the Cr sites. Using the classical Heisenberg model,

$$H = \sum_{ij} J_{ij} \mathbf{S}_i \cdot \mathbf{S}_j, \tag{1}$$

is justified by the negligibly small magnetocrystalline anisotropy [8–10]. Thus, we consider throughout the paper $J_{ij} \equiv J_n$ if sites i and j are nth neighbors [see Fig. 1(a)]. Depending on the chemical composition, chromium spinels exhibit different mechanisms of frustration, such as geometric frustration that occurs if dominant NN interactions are antiferromagnetic, or bond frustration, which originates from competition between ferromagnetic NN and antiferromagnetic further-neighbor exchange.

To estimate the range and relative strengths of coupling constants J_n in chromium spinels, Yaresko [7] performed *ab initio* calculations to extract exchange parameters up to the fourth nearest neighbor for various compounds of this family. Calculations showed that the NN interaction J_1 changes gradually from antiferromagnetic in some oxides to ferromagnetic in sulfides and selenides, while the next-nearest-neighbor (NNN) interaction J_2 is noticeably weaker than the antiferromagnetic J_3 exchange parameter (see Table I). For the $HgCr_2O_4$ system, J_1 can be even weaker than J_2 (or comparable, depending on the effective Coulomb repulsion U), so that the third-nearest-neighbor interaction J_3 may become dominant. Therefore, the existing theoretical phase diagram restricted to only NN and NNN interactions [3] appears insufficient for a realistic description of these materials. The importance of the two third-nearest-neighbor exchange paths on the pyrochlore lattice has also been emphasized for the spin-1/2 molybdate Heisenberg antiferromagnet $Lu_2Mo_2O_5N_2$ [11], where J_3' and J_3'' have opposite signs and dominate over J_2. It was recently conjectured that this may lead to an unusual "gearwheel" type of a quantum spin liquid [12].

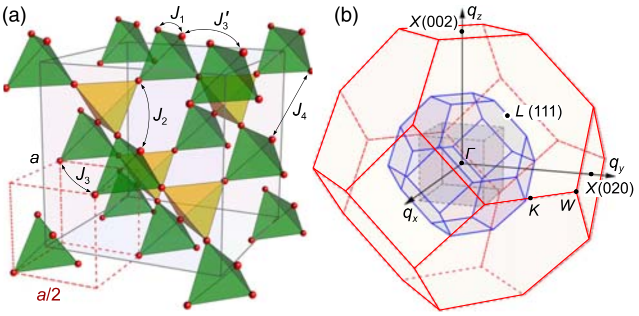

FIG. 1. (a) Pyrochlore-lattice structure, representative of the magnetic Cr sublattice in ACr_2X_4 spinels. Small spheres represent Cr^{3+} ions. The pyrochlore lattice can be described either as an fcc arrangement of separated Cr_4 tetrahedra formed by NN bonds (large cubic unit cell, solid lines) or as a half filled fcc lattice of Cr^{3+} ions with a twice smaller lattice parameter (small cubic unit cell, dashed lines). We also show different exchange paths corresponding to $J_1 \ldots J_4$ interactions that are discussed in the text. (b) The simple-cubic Brillouin zone with dimensions $2\pi/a$ (central cube), and the two unfolded Brillouin zones corresponding to fcc lattices with parameters a and $a/2$ (truncated octahedra). The high-symmetry points are marked according to the large unfolded zone.

B. Classical phase diagram relevant for chromium spinels

An inspection of the theoretically predicted exchange parameters for various ACr_2X_4 spinels presented in Ref. [7] reveals non-negligible exchange integrals up to the fourth-nearest neighbor, J_4, which is ferromagnetic in all the studied compounds. The third-nearest-neighbor exchange constants are, on the other hand, antiferromagnetic. Note that the pyrochlore lattice exhibits two inequivalent sets of third-nearest neighbors. Following Ref. [7], we treat their corresponding exchange couplings as equal, $J_3' = J_3'' \equiv J_3$, since deviations are considered to be small. The classical ground state depends only on the ratios between the exchange constants, which can be much more accurately predicted in first-principles calculations than their absolute values. Here we restrict our attention to the sulfides, selenides, and $HgCr_2O_4$ with ferromagnetic NN interactions, $J_1 < 0$. In Table I, we summarize the calculated ratios $J_2/|J_1|$, $J_3/|J_1|$, and $J_4/|J_1|$ for all seven compounds considered in Ref. [7] (to be specific, we list the ratios for LSDA + U with $U = 2$ eV), along with their experimentally determined ground states.

We determine the classical phase diagram by means of a direct energy minimization scheme [3]. We consider a pyrochlore lattice (periodic boundary conditions imposed)

TABLE I. Ratios of the exchange constants in different chromium spinels after Ref. [7], taken for a moderate effective Coulomb repulsion $U = 2$ eV. For each compound, its experimentally measured ground state is also given: antiferromagnetic (AFM), ferromagnetic (FM), or proper-screw spin spiral. The bottom row shows experimental values for $ZnCr_2Se_4$ estimated from our INS data in Sec. II. B.

Compound	$J_2/\lvert J_1\rvert$	$J_3/\lvert J_1\rvert$	$J_4/\lvert J_1\rvert$	Ground state	References
$HgCr_2O_4$	0.1714	0.471	0	AFM	[13]
$ZnCr_2S_4$	0.0395	0.198	−0.014	(00q) spiral	[14]
$CdCr_2S_4$	0.0065	0.116	−0.015	FM	[15]
$HgCr_2S_4$	0.0222	0.111	−0.013	(00q) spiral	[16,17]
$ZnCr_2Se_4$	0.0102	0.169	−0.018	(00q) spiral	[18,19]
$CdCr_2Se_4$	−0.0071	0.101	−0.013	FM	[15]
$HgCr_2Se_4$	−0.0014	0.109	−0.013	FM	[20]
Experimental values					
$ZnCr_2Se_4$	0.0118	0.170	−0.014		[This work]

with typically $L = 8$ unit cells (containing 16 spins) in each spatial direction, resulting in $N = 16L^3 = 2^{13}$ spins in total. Starting from a random initial spin configuration, one randomly picks a lattice site i and rotates its spin $\mathbf{S}_i$ antiparallel to its local field defined as $\mathbf{h}_i = \partial H/\partial \mathbf{S}_i = \sum_{j\neq i} J_{ij}\mathbf{S}_j$, thereby minimizing the energy and simultaneously keeping the spins normalized. Once an energetically minimal spin configuration has been found, the object of interest is the spin structure factor $\mathcal{S}(\mathbf{q}) = \frac{1}{N}|\sum_j \mathbf{S}_j \exp(i\mathbf{q}\cdot\mathbf{r}_j)|^2$ with its magnetic Bragg peaks.

The pure J_1-J_2 phase diagram has already been computed [3]. As mentioned before, we consider only ferromagnetic J_1. Table I reveals that the couplings J_4 of all considered spinels are ferromagnetic and roughly equal, $J_4/|J_1| \approx -0.014$ (which also corresponds to the value determined by fitting the experimental data to spin-wave excitation spectra; see Sec. II. B). Thus, we restrict our investigation of the phase diagram to $J_4/|J_1| = -0.014$, but we have checked for all spinels that the ground state remains unchanged when taking into account the couplings listed in Table I. Therefore, we map out the classical phase diagram for $-0.05 \leq J_2/|J_1| \leq 0.2$ and $0 \leq J_3/|J_1| \leq 0.5$ as presented in Fig. 2. We find five different phases: ferromagnetic (FM), $(00q)$ proper-screw spiral, cuboctahedral stack (CS), multiply modulated commensurate spiral (MMCS), and the $(\frac{1}{8}\frac{1}{2}\frac{7}{8})$ phase. Quite generally, we observe for $J_2/|J_1| > 0.1$ and $J_3/|J_1| > 0.1$ that the energy landscape becomes extremely flat. In order to yield reliable results we had to increase system sizes drastically; for some parameter settings we even used $L = 32$ corresponding to more than half a million spins. For dominant $J_1 < 0$, we find FM order, but both antiferromagnetic J_2 and J_3 destabilize the phase. For sufficiently strong $J_3 > 0$ (and not too large J_2) there is a phase transition from the FM to the $(00q)$ helical phase. The wave vector q changes continuously from the phase transition line ($q = 0$) up to a maximal value of $q = 7/8$ for large J_3 (color coded in increments of $q = 1/8$ in Fig. 2). For $J_3 = 0$ and $J_2/|J_1| \geq 0.2$, we find the CS phase of Ref. [3] characterized by Bragg peaks at three of the four $\{\frac{1}{2}\frac{1}{2}\frac{1}{2}\}$-type $\mathbf{q}$ vectors. Finite J_3 stabilizes the phase down to smaller values of J_2. Further increase of J_3 drives the system into the multi-$\mathbf{q}$ MMCS phase, which is also present in a very small parameter range of the J_1-J_2 phase diagram [3]. This state is characterized by four main Bragg peaks at $(\frac{1}{4}\frac{3}{4}\frac{1}{2})$, $(\frac{3}{4}\frac{1}{4}\frac{1}{2})$, $(\frac{1}{4}\frac{3}{4}\frac{3}{2})$, and $(\frac{3}{4}\frac{1}{4}\frac{3}{2})$, and a subdominant peak at $(\frac{3}{4}\frac{3}{4}0)$ (or symmetry-related combinations of these vectors, respectively). Making J_3 even larger eventually turns the system's ground state into an exotic phase with four dominant magnetic Bragg peaks at $\mathbf{q} = (\pm\frac{1}{8}\ \frac{1}{2}\ \pm\frac{7}{8})$ and $(\pm\frac{7}{8}\ \frac{1}{2}\ \pm\frac{1}{8})$. To the best of our knowledge, this phase has not been mentioned before in the literature, and we simply call it the $(\frac{1}{8}\frac{1}{2}\frac{7}{8})$ phase.

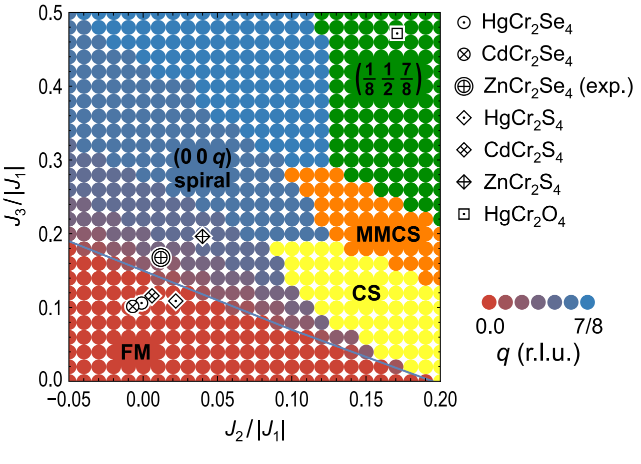

FIG. 2. Classical J_2-J_3 phase diagram for $J_1 = -1$ and $J_4/|J_1| = -0.014$ containing five phases: ferromagnetic (FM), $(00q)$ proper-screw spiral with the corresponding q value shown in color code, the cuboctahedral stack (CS), the multiply modulated commensurate spiral (MMCS), and the $(\frac{1}{8}\frac{1}{2}\frac{7}{8})$ phase. In addition, the location of the seven spinel compounds with ferromagnetic J_1 is indicated by the symbols. For details, see the text and Table I.

The phase diagram in Fig. 2 contains all spinels listed in Table I, and it is interesting to compare the results of our calculations with available experimental data. $CdCr_2S_4$, $HgCr_2Se_4$, and $CdCr_2Se_4$ have been reported to possess ferromagnetic ground states [15,20] in agreement with our simulations. $HgCr_2S_4$ develops a $(00q)$ spiral configuration with a temperature-dependent pitch [16], but the experimental results emphasize a strong tendency to ferromagnetic correlations [17]; in our phase diagram it is located in the FM phase close to the spiral phase. The material of highest interest is, of course, $ZnCr_2Se_4$, where both experiment and simulation consistently find a $(00q)$ helix with $q = 0.468$ r.l.u. (or 0.28 Å^{-1}). $ZnCr_2S_4$ has been reported to host a similar proper-screw spin structure in the temperature range $8\ \mathrm{K} < T < 15\ \mathrm{K}$, with $q = 0.787$ [14], which agrees fairly well with our simulated value $q = 0.625$ based on the coupling constants from Table I. This spinel undergoes a structural phase transition at 8 K with a change of the magnetic order. The only oxide in our list is $HgCr_2O_4$, where Bragg peaks corresponding to $\mathbf{q}_1 = (100)$ and $\mathbf{q}_2 = (10\frac{1}{2})$ were measured [13]. The compound undergoes, however, a structural phase transition into an orthorhombic phase [21] for which our pyrochlore description is, of course, inadequate. Otherwise, according to its exchange couplings, $HgCr_2O_4$ would be located in the $(\frac{1}{8}\frac{1}{2}\frac{7}{8})$ phase.

We emphasize that our phase diagram, based on the *ab initio* parameters of Ref. [7], agrees fairly well with the available experimental results. The major discrepancies are associated with structural transitions of the spinels $ZnCr_2S_4$ and $HgCr_2O_4$, leading to distortions or even different crystal structure. Since both effects cannot be captured by our simulations, the discrepancies between experiment